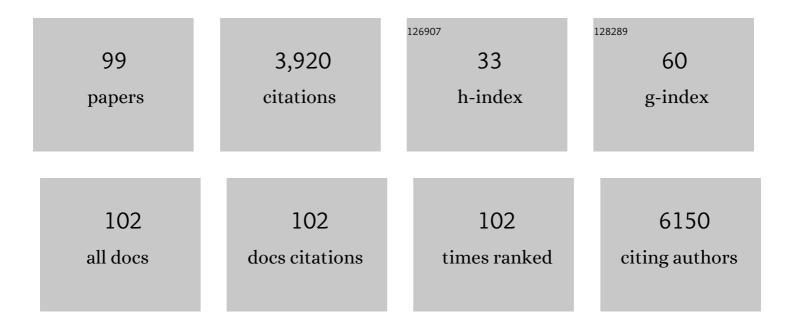
Jun Zhu

List of Publications by Year in descending order

Source: https://exaly.com/author-pdf/1316597/publications.pdf Version: 2024-02-01



Іны 7нн

#	Article	IF	CITATIONS
1	Recent progress in inorganic tin perovskite solar cells. Materials Today Energy, 2022, 23, 100891.	4.7	16
2	Roles of micro-aeration on enhancing volatile fatty acids and lactic acid production from agricultural wastes. Bioresource Technology, 2022, 347, 126656.	9.6	9
3	Over 8% efficient CsSnI ₃ -based mesoporous perovskite solar cells enabled by two-step thermal annealing and surface cationic coordination dual treatment. Journal of Materials Chemistry A, 2022, 10, 3642-3649.	10.3	35
4	Ultrathin SnO ₂ Buffer Layer Aids in Interface and Band Engineering for Sb ₂ (S,Se) ₃ Solar Cells with over 8% Efficiency. ACS Applied Energy Materials, 2022, 5, 3022-3033.	5.1	13
5	Guanidinium Thiocyanate Additive Engineering for High-Performance CsPblBr ₂ Solar Cells with an Efficiency of 10.90%. ACS Applied Energy Materials, 2022, 5, 3110-3118.	5.1	8
6	SnO ₂ Quantum Dot-Modified Mesoporous TiO ₂ Electron Transport Layer for Efficient and Stable Perovskite Solar Cells. ACS Applied Energy Materials, 2022, 5, 3052-3063.	5.1	18
7	Ligand-mediated CsPbBr _x I _{3â^'} _x /SiO ₂ quantum dots for red, stable and low-threshold amplify spontaneous emission. Nanotechnology, 2022, 33, 285201.	2.6	2
8	Produce individual medium chain carboxylic acids (MCCA) from swine manure: Performance evaluation and economic analysis. Waste Management, 2022, 144, 255-262.	7.4	4
9	A nanofibrillar conjugated polymer film as an interface layer for high-performance CsPblBr ₂ solar cells with efficiency exceeding 11%. Sustainable Energy and Fuels, 2022, 6, 2692-2699.	4.9	4
10	Optimization of a dual-chamber electrolytic reactor with a magnesium anode and characterization of struvite produced from synthetic wastewater. Environmental Technology (United Kingdom), 2022, , 1-37.	2.2	2
11	Start-up of co-digestion of poultry litter and wheat straw in anaerobic sequencing batch reactor by gradually increasing organic loading rate: Methane production and microbial community analysis. Bioresource Technology, 2022, 354, 127232.	9.6	16
12	ZnI ₂ post-processing of CsPbBr ₃ quantum dots for red, stable, and low-threshold amplified spontaneous emission. Applied Physics Letters, 2022, 120, 221101.	3.3	0
13	VOC over 1.2ÂV for Cs2AgBiBr6 solar cells based on formamidinium acetate additive. Journal of Materials Science: Materials in Electronics, 2022, 33, 18758-18767.	2.2	9
14	The phosphohistidine phosphatase SixA dephosphorylates the phosphocarrier NPr. Journal of Biological Chemistry, 2021, 296, 100090.	3.4	2
15	Effects of Regulatory Network Organization and Environment on PmrD Connector Activity and Polymyxin Resistance in <i>Klebsiella pneumoniae</i> and <i>Escherichia coli</i> . Antimicrobial Agents and Chemotherapy, 2021, 65, .	3.2	9
16	Phosphatidic acid-mediated binding and mammalian cell internalization of the Vibrio cholerae cytotoxin MakA. PLoS Pathogens, 2021, 17, e1009414.	4.7	8
17	Gapless Spin Wave Transport through a Quantum Canted Antiferromagnet. Physical Review X, 2021, 11, .	8.9	15
18	Regulating the Film Growth and Reducing the Defects for Efficient CsPbIBr ₂ Solar Cells. ACS Applied Materials & Interfaces, 2021, 13, 24654-24661.	8.0	21

#	Article	IF	CITATIONS
19	Contributions of Escherichia coli and Its Motility to the Formation of Dual-Species Biofilms with Vibrio cholerae. Applied and Environmental Microbiology, 2021, 87, e0093821.	3.1	9
20	Effects of the doping density of charge-transporting layers on regular and inverted perovskite solar cells: numerical simulations. Advanced Composites and Hybrid Materials, 2021, 4, 1146-1154.	21.1	27
21	Enhancing the performance of CsPbIBr2 solar cells through zinc halides doping. Synthetic Metals, 2021, 281, 116918.	3.9	5
22	Strontiumâ€Doped CsPbI ₃ Quantum Dots as an Interfacial Layer for Efficient Inorganic Perovskite Solar Cells. Solar Rrl, 2021, 5, .	5.8	12
23	Effect of Pretreatment on Hydraulic Performance of the Integrated Membrane Process for Concentrating Nutrient in Biogas Digestate from Swine Manure. Membranes, 2020, 10, 249.	3.0	9
24	Study on removal of phosphorus as struvite from synthetic wastewater using a pilot-scale electrodialysis system with magnesium anode. Science of the Total Environment, 2020, 726, 138221.	8.0	25
25	Solution-processed polarized light-emitting diodes. Journal of Materials Chemistry C, 2020, 8, 9147-9162.	5.5	5
26	CsPbBr ₃ nanowire polarized light-emitting diodes through mechanical rubbing. Chemical Communications, 2020, 56, 5413-5416.	4.1	25
27	Vibrio cholerae Virulence Activator ToxR Regulates Manganese Transport and Resistance to Reactive Oxygen Species. Infection and Immunity, 2020, 88, .	2.2	3
28	Hydrogen and methane production by co-digesting liquid swine manure and brewery wastewater in a two-phase system. Bioresource Technology, 2019, 293, 122041.	9.6	24
29	Template deposition of Sb2S3 for solid-state sensitized solar cells. Journal of Alloys and Compounds, 2019, 784, 947-953.	5.5	17
30	Black soldier fly larvae (<i>Hermetia illucens</i>) strengthen the metabolic function of food waste biodegradation by gut microbiome. Microbial Biotechnology, 2019, 12, 528-543.	4.2	127
31	Odor removal by and microbial community in the enhanced landfill cover materials containing biochar-added sludge compost under different operating parameters. Waste Management, 2019, 87, 679-690.	7.4	37
32	Colistin Resistance-Mediated Bacterial Surface Modification Sensitizes Phage Infection. Antimicrobial Agents and Chemotherapy, 2019, 63, .	3.2	19
33	Sb ₂ S ₃ solar cells: functional layer preparation and device performance. Inorganic Chemistry Frontiers, 2019, 6, 3381-3397.	6.0	33
34	Anaerobic co-digestion of poultry litter and wheat straw affected by solids composition, free ammonia and carbon/nitrogen ratio. Journal of Environmental Science and Health - Part A Toxic/Hazardous Substances and Environmental Engineering, 2019, 54, 231-237.	1.7	12
35	CitAB Two-Component System-Regulated Citrate Utilization Contributes to <i>Vibrio cholerae</i> Competitiveness with the Gut Microbiota. Infection and Immunity, 2019, 87, .	2.2	19
36	The SOS Response Mediates Sustained Colonization of the Mammalian Gut. Infection and Immunity, 2019, 87, .	2.2	17

#	Article	lF	CITATIONS
37	An ultrathin SiO2 blocking layer to suppress interfacial recombination for efficient Sb2S3-sensitized solar cells. Inorganic Chemistry Frontiers, 2018, 5, 1370-1377.	6.0	12
38	A Bi-functional additive for linking PI 2 and decreasing defects in organo-halide perovskites. Journal of Alloys and Compounds, 2018, 758, 171-176.	5.5	12
39	Pre-digestion to enhance volatile fatty acids (VFAs) concentration as a carbon source for denitrification in treatment of liquid swine manure. Journal of Environmental Science and Health - Part A Toxic/Hazardous Substances and Environmental Engineering, 2018, 53, 891-898.	1.7	6
40	Solution-processed CuSbS2 solar cells based on metal–organic molecular solution precursors. Journal of Materials Science, 2018, 53, 2016-2025.	3.7	29
41	Facile fabrication of perovskite layers with large grains through a solvent exchange approach. Inorganic Chemistry Frontiers, 2018, 5, 348-353.	6.0	34
42	Modeling Power Generation and Energy Efficiencies in Air-Cathode Microbial Fuel Cells Based on Freter Equations. Applied Sciences (Switzerland), 2018, 8, 1983.	2.5	9
43	A valley valve and electron beam splitter. Science, 2018, 362, 1149-1152.	12.6	106
44	Triple cation additive NH ₃ ⁺ C ₂ H ₄ NH ₂ ⁺ C ₂ phase-stable inorganic α-CsPbI ₃ perovskite films for use in solar cells. Journal of Materials Chemistry A, 2018, 6, 18258-18266.	H _{4<}	/sub>NH <sub< td=""></sub<>
45	Modeling Kinetics of Anaerobic Co-Digestion of Poultry Litter and Wheat Straw Mixed with Municipal Wastewater in a Continuously Mixed Digester with Biological Solid Recycle Using Batch Experimental Data. Chemical Engineering Communications, 2017, 204, 501-511.	2.6	5
46	Identification and characterization of a new intermediate to obtain high quality perovskite films with hydrogen halides as additives. Inorganic Chemistry Frontiers, 2017, 4, 473-480.	6.0	23
47	Temperature-assisted rapid nucleation: a facile method to optimize the film morphology for perovskite solar cells. Journal of Materials Chemistry A, 2017, 5, 20327-20333.	10.3	148
48	Feeding schemes and C/N ratio of a laboratory-scale step-fed sequencing batch reactor for liquid swine manure treatment. Journal of Environmental Science and Health - Part A Toxic/Hazardous Substances and Environmental Engineering, 2017, 52, 718-726.	1.7	3
49	Incorporating Graphitic Carbon Nitride (gâ€C ₃ N ₄) Quantum Dots into Bulkâ€Heterojunction Polymer Solar Cells Leads to Efficiency Enhancement. Advanced Functional Materials, 2016, 26, 1719-1728.	14.9	221
50	Quasi-solid-state dye-sensitized solar cell based on gel electrolyte with high gel to solution transition temperature using low molecular mass organogelator. Journal of Photochemistry and Photobiology A: Chemistry, 2016, 329, 139-145.	3.9	8
51	Kinetics of batch anaerobic co-digestion of poultry litter and wheat straw including a novel strategy of estimation of endogenous decay and yield coefficients using numerical integration. Bioprocess and Biosystems Engineering, 2016, 39, 1553-1565.	3.4	10
52	A new probe into thin copper sulfide counter electrode with thickness below 100 nm for quantum dot-sensitized solar cells. Electrochimica Acta, 2016, 205, 45-52.	5.2	7
53	Modified surface loading process for achieving improved performance of the quantum dot-sensitized solar cells. Chemical Physics Letters, 2016, 653, 173-177.	2.6	2
54	Scalable noninjection phosphine-free synthesis and optical properties of tetragonal-phase CuInSe2quantum dots. Nanoscale, 2016, 8, 10021-10025.	5.6	14

#	Article	IF	CITATIONS
55	Ligand-free nano-grain Cu ₂ SnS ₃ as a potential cathode alternative for both cobalt and iodine redox electrolyte dye-sensitized solar cells. Journal of Materials Chemistry A, 2016, 4, 14865-14876.	10.3	21
56	Metagenomic analysis of microbiota structure evolution in phytoremediation of a swine lagoon wastewater. Bioresource Technology, 2016, 219, 439-444.	9.6	61
57	Effect of the self-assembled gel network formed from a low molecular mass organogelator on the electron kinetics in quasi-solid-state dye-sensitized solar cells. Science China Materials, 2016, 59, 787-796.	6.3	4
58	Plant nodulation inducers enhance horizontal gene transfer of <i>Azorhizobium caulinodans</i> symbiosis island. Proceedings of the National Academy of Sciences of the United States of America, 2016, 113, 13875-13880.	7.1	82
59	Semiconductor Sensitized Solar Cells Based on BiVO4-Sensitized Mesoporous SnO2 Photoanodes. Journal of Nanoscience and Nanotechnology, 2016, 16, 5719-5723.	0.9	1
60	Optimization of methane production in anaerobic co-digestion of poultry litter and wheat straw at different percentages of total solid and volatile solid using a developed response surface model. Journal of Environmental Science and Health - Part A Toxic/Hazardous Substances and Environmental Engineering, 2016, 51, 325-334.	1.7	23
61	Credible evidence for the passivation effect of remnant Pbl ₂ in CH ₃ NH ₃ Pbl ₃ films in improving the performance of perovskite solar cells. Nanoscale, 2016, 8, 6600-6608.	5.6	86
62	TiO ₂ Sub-microsphere Film as Scaffold Layer for Efficient Perovskite Solar Cells. ACS Applied Materials & Interfaces, 2016, 8, 8162-8167.	8.0	44
63	Kinetics, equilibrium, and thermodynamics of ammonium sorption from swine manure by natural chabazite. Separation Science and Technology, 2016, 51, 202-213.	2.5	20
64	Influence of Insulating Oxide Coatings on the Performance of Perovskite Solar Cells and the Interface Charge Recombination Dynamics. Wuli Huaxue Xuebao/ Acta Physico - Chimica Sinica, 2016, 32, 1207-1213.	4.9	0
65	Efficiency Enhancement of Inverted Structure Perovskite Solar Cells via Oleamide Doping of PCBM Electron Transport Layer. ACS Applied Materials & Interfaces, 2015, 7, 13659-13665.	8.0	132
66	Earth-abundant Cu2SnSe3 thin film counter electrode for high-efficiency quantum dot-sensitized solar cells. Journal of Power Sources, 2015, 292, 7-14.	7.8	40
67	Kesterite Cu ₂ ZnSnS ₄ as a Low-Cost Inorganic Hole-Transporting Material for High-Efficiency Perovskite Solar Cells. ACS Applied Materials & Interfaces, 2015, 7, 28466-28473.	8.0	147
68	Low-temperature, solution-deposited metal chalcogenide films as highly efficient counter electrodes for sensitized solar cells. Journal of Materials Chemistry A, 2015, 3, 6315-6323.	10.3	80
69	Improving the Conductivity of PEDOT:PSS Hole Transport Layer in Polymer Solar Cells via Copper(II) Bromide Salt Doping. ACS Applied Materials & Interfaces, 2015, 7, 1439-1448.	8.0	76
70	SnX (X = S, Se) thin films as cost-effective and highly efficient counter electrodes for dye-sensitized solar cells. Chemical Communications, 2015, 51, 8108-8111.	4.1	46
71	Mesoporous SnO ₂ nanoparticle films as electron-transporting material in perovskite solar cells. RSC Advances, 2015, 5, 28424-28429.	3.6	154
72	Quasi-solid-state dye sensitized solar cells using supramolecular gel electrolyte formed from two-component low molecular mass organogelators. Science China Materials, 2015, 58, 447-454.	6.3	8

#	Article	IF	CITATIONS
73	Colloidal CuInS ₂ Quantum Dots as Inorganic Hole-Transporting Material in Perovskite Solar Cells. ACS Applied Materials & Interfaces, 2015, 7, 17482-17488.	8.0	119
74	Efficient inorganic solid solar cells composed of perovskite and PbS quantum dots. Nanoscale, 2015, 7, 9902-9907.	5.6	73
75	Influence of temperature on the single-stage ATAD process predicted by a thermal equilibrium model. Journal of Environmental Management, 2015, 156, 257-265.	7.8	4
76	Determination of the optimal dosing time of ferric nitrate on disinhibition of excessive volatile fatty acids in autothermal thermophilic aerobic digestion for sewage sludge. RSC Advances, 2015, 5, 43949-43955.	3.6	5
77	A novel polysulfide hydrogel electrolyte based on low molecular mass organogelator for quasi-solid-state quantum dot-sensitized solar cells. Journal of Power Sources, 2015, 284, 582-587.	7.8	40
78	BiVO4 semiconductor sensitized solar cells. Science China Chemistry, 2015, 58, 1489-1493.	8.2	17
79	Effect of alkyl chain length of imidazolium cations on the electron transport and recombination kinetics in ionic gel electrolytes based quasi-solid-state dye-sensitized solar cells. Electrochimica Acta, 2015, 168, 313-319.	5.2	14
80	Effects of stabilization and sludge properties in a combined process of anaerobic digestion and thermophilic aerobic digestion. Environmental Technology (United Kingdom), 2015, 36, 2786-2795.	2.2	5
81	High-efficiency and stable quasi-solid-state dye-sensitized solar cell based on low molecular mass organogelator electrolyte. Journal of Materials Chemistry A, 2015, 3, 2344-2352.	10.3	91
82	Enhanced electrocatalytic activity of vacuum thermal evaporated Cu x S counter electrode for quantum dot-sensitized solar cells. Electrochimica Acta, 2015, 154, 47-53.	5.2	15
83	CdS and CdSe quantum dot co-sensitized nanocrystalline TiO2 electrode: Quantum dot distribution, thickness optimization, and the enhanced photovoltaic performance. Journal of Power Sources, 2015, 273, 645-653.	7.8	39
84	1D Coâ€Pi Modified BiVO ₄ /ZnO Junction Cascade for Efficient Photoelectrochemical Water Cleavage. Advanced Energy Materials, 2014, 4, 1301590.	19.5	226
85	Ex Situ CdSe Quantum Dot-Sensitized Solar Cells Employing Inorganic Ligand Exchange To Boost Efficiency. Journal of Physical Chemistry C, 2014, 118, 214-222.	3.1	44
86	lsopropanol-treated PEDOT:PSS as electron transport layer in polymer solar cells. Organic Electronics, 2014, 15, 3445-3451.	2.6	39
87	Gel electrolyte materials formed from a series of novel low molecular mass organogelators for stable quasi-solid-state dye-sensitized solar cells. Journal of Materials Chemistry A, 2014, 2, 15921-15930.	10.3	19
88	Clostridium difficile contains plasmalogen species of phospholipids and glycolipids. Biochimica Et Biophysica Acta - Molecular and Cell Biology of Lipids, 2014, 1841, 1353-1359.	2.4	32
89	Stable Quasi-Solid-State Dye-Sensitized Solar Cells Using Novel Low Molecular Mass Organogelators and Room-Temperature Molten Salts. Journal of Physical Chemistry C, 2014, 118, 16718-16726.	3.1	37
90	Numerical simulation: Toward the design of high-efficiency planar perovskite solar cells. Applied Physics Letters, 2014, 104, .	3.3	232

#	Article	IF	CITATIONS
91	Stable quasi-solid-state dye-sensitized solar cell using a diamide derivative as low molecular mass organogelator. Journal of Power Sources, 2014, 262, 444-450.	7.8	20
92	Optimization of continuous hydrogen production from co-fermenting molasses with liquid swine manure in an anaerobic sequencing batch reactor. Bioresource Technology, 2013, 136, 351-359.	9.6	26
93	Optimization of single-crystal rutile TiO2 nanorod arrays based dye-sensitized solar cells and their electron transport properties. Journal of Power Sources, 2013, 235, 193-201.	7.8	43
94	SnSe2 quantum dot sensitized solar cells prepared employing molecular metal chalcogenide as precursors. Chemical Communications, 2012, 48, 3324.	4.1	67
95	The optical and electrochemical properties of CdS/CdSe co-sensitized TiO2 solar cells prepared by successive ionic layer adsorption and reaction processes. Solar Energy, 2012, 86, 964-971.	6.1	80
96	Effects of Hydrothermal Growth Conditions of ZnO Nanorods Arrays on Flexible Dye-sensitized Solar Cells. Wuji Cailiao Xuebao/Journal of Inorganic Materials, 2012, 27, 775-779.	1.3	4
97	Thermal Annealing Effects on the Absorption and Structural Properties of Regioregular Poly(3-Hexylthiophene) Films. Journal of Macromolecular Science - Physics, 2011, 50, 624-636.	1.0	14
98	Effect of pH on continuous biohydrogen production from liquid swine manure with glucose supplement using an anaerobic sequencing batch reactor. International Journal of Hydrogen Energy, 2010, 35, 6592-6599.	7.1	54
99	Biogas and CH4 productivity by co-digesting swine manure with three crop residues as an external carbon source. Bioresource Technology, 2010, 101, 4042-4047.	9.6	205